PII: S0032-3861(97)00351-0

Polymer Vol. 38 No. 26, pp. 6427–6430, 1997

0032-3861/97/$17.00+0.00

A simultaneous SAXS/WAXS and stress–strain study of polyethylene deformation at high strain rates

D. J. Hughes[a], **A. Mahendrasingam**[a], **W. B. Oatway**[a], **E. L. Heeley**[a], **C. Martin**[a] **and W. Fuller**[a,*]
[a]*Department of Physics, Keele University, Keele, Staffs. ST5 5BG, UK*
(Revised 21 April 1997)

An experimental system has been commissioned which allows the collection of time-resolved simultaneous two-dimensional small-angle X-ray scattering/wide-angle X-ray scattering (SAXS/WAXS) and stress–strain data with a temporal resolution of 40 ms during the drawing of synthetic polymers. X-ray data collection is achieved via two CCD-based area detectors which are positioned in order to maximize the amount of scattering that can be observed from a particular sample. True stress–strain measurements are obtained from video extensometer and load cell measurements. The system was used at the Daresbury SRS to study the structural changes which occur in a sample of isotropic high-density polyethylene when subjected to an overall strain rate of $\approx 3\ \mathrm{s}^{-1}$. It is shown that the onset of both a partial stress-induced crystal phase change and micro-voiding in the sample can be directly correlated to the point of yield in the true stress–strain curve. © 1997 Elsevier Science Ltd.

(Keywords: SAXS/WAXS; deformation; polyethylene)

Introduction

Since the solution of the orthorhombic crystal structure of polyethylene by Bunn[1] nearly sixty years ago, both the morphology and the deformation behaviour of this commercially important thermoplastic have been extensively studied. It has been shown both theoretically and experimentally that when polyethylene is subjected to an applied load, a number of deformation mechanisms are possible[2–4]. The modes of deformation can be considered both on a crystallographic scale (slip, twinning and a Martensitic transformation), and at a lamellar level (interlamellar shear, interlamellar separation and stack rotation). However, the extent to which each of these competing processes contribute to the overall deformation in bulk polyethylene is not yet fully understood. Furthermore, the dominance of a particular mechanism is significantly affected by various factors such as degree of chain branching, molecular weight, deformation rate and deformation temperature.

Wide-angle X-ray scattering (WAXS) and small-angle X-ray scattering (SAXS) are both powerful tools that have been used to study the complex morphological changes that occur in polyethylene during deformation[5,6]. However in recent years, with the availability of high brilliance synchrotron X-ray sources, there has been a trend towards the simultaneous collection of both SAXS and WAXS data[7,8]. Advances in detector technology have lead to more rapid data collection allowing in-situ measurements to be made during the deformation of organic polymers.

A system has recently been developed by the Keele fibre diffraction group[9], which allowed the collection of high-resolution two-dimensional simultaneous SAXS/WAXS data during the drawing of polyethylene. This system was based around a CCD-based area detector for the collection of WAXS data, and a gas-filled multiwire area detector for the collection of SAXS data. The main limitation of this system was that a relatively low data collection rate was achievable because of the maximum count rate limitations of the multiwire detector. In order to overcome this problem we have commissioned a second CCD-based area detector for the collection of SAXS data. This now allows us to collect a series of accurately synchronized two-dimensional SAXS/WAXS data with a temporal resolution of up to 40 ms.

There is a great need to correlate not only the wide-angle and small-angle X-ray scattering data, but also data describing the mechanical yield of the sample under observation. Since deformation is rarely homogeneous, it is essential that these measurements are performed in situ if they are to allow accurate characterisation of the dynamic processes that occur during drawing. Video extensometry has been used by a number of groups in order to record accurate strain and sample cross-section data during deformation of a sample[10,11]. We have incorporated this technique so that we can obtain sample video data simultaneously with the X-ray scattering data. Furthermore, a cell has been constructed so that simultaneous sample loading data may also be collected. Using these techniques, it is possible for the first time to accurately correlate both the WAXS and SAXS data with specific points upon the stress–strain curve at high strain rates.

Experimental

A drawing camera has been constructed in the Keele Physics Department workshop[12] which allows the deformation of synthetic polymer samples at temperatures from ambient to 350°C and at rates up to $12\ \mathrm{s}^{-1}$ [13]. The camera has been specifically modified in order to allow the collection of both SAXS and WAXS data. The sample environment consists of a $150 \times 150 \times 150\ \mathrm{mm}^3$ oven with two vertically opposed stepper-motor-driven jaws. The sample under investigation is positioned between these jaws prior to uniaxial deformation. WAXS and SAXS data exit the camera via a thin aluminium window ($\approx 15\ \mu\mathrm{m}$). In order to eliminate strong reflections in the WAXS data due to the main beam scattering from this window, a 13 mm diameter,

---

* To whom correspondence should be addressed

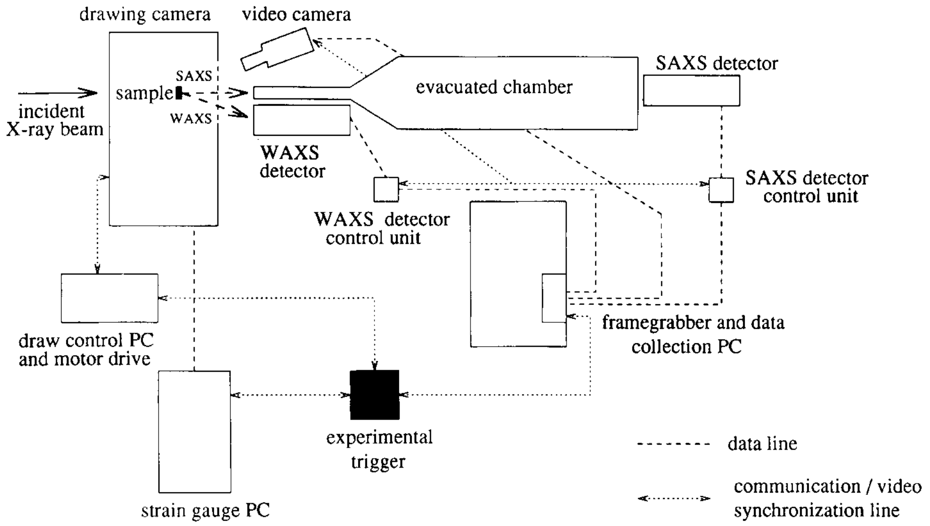

Figure 1 Schematic representation of the experimental arrangement that was used at station 16.1 of the Daresbury SRS. Data lines from the SAXS/WAXS detectors and video camera to the data collection PC are shown, as are the electronic lines needed to ensure accurate synchronisation between the data

15 μm thick mica disc is used to cover a hole cut in the window at the main beam position.

The two X-ray area detectors were purchased from Photonic Science Ltd. Both detectors are of a similar design, having a gadolinium oxysulphide scintillator which is fibre optically coupled to an image intensified CCD. The output from each detector is in the form of a standard CCIR video signal with a frame rate of 25 s^{-1}. In order to convert the video data into standard 8-bit binary data, a powerful Synoptics i860 processor based video framegrabber, controlled by an IBM compatible PC is used. This frame grabber has 128 MB of on board memory and can simultaneously digitize up to three video signals with no loss of data.

The experiments reported here were performed on experimental station 16.1 of the Daresbury SRS. *Figure 1* shows a schematic representation of the experimental arrangement. An evacuated beampipe is placed between the exit from the drawing camera and the SAXS detector in order to minimise air scatter in the SAXS data. In order to maximise the extent of wide-angle data that could be collected, the WAXS detector and evacuated beampipe entrance have been specifically designed so that the detector may be positioned very close to the main beam without actually impinging upon the SAXS data. The detective area of both the SAXS and WAXS detectors are normal to the main beam. The video data from both detectors is connected to the first two inputs of the video framegrabber.

Strain information was recorded simultaneously during the draw via a commercially available CCD video camera with a macro-focusing telephoto lens. The output from this video camera was fed into the third input of the video framegrabber. It is this data collection methodology which ensures that the SAXS, WAXS and video strain data are accurately synchronized. A bridge-type strain gauge cell was constructed and interfaced to a data collection PC, so that the physical loading across the sample during the draw could be recorded.

The key to multiple technique experiments such as the experiment detailed here, is to ensure accurate synchronization between the various sets of data. Accurate synchronization is of an even greater importance in an experiment where the data is to be resolved at a temporal resolution of 40 ms. In order to obtain sufficient synchronization, an electronic experimental trigger was constructed which provides accurate timing of the initiation of data collection for both the SAXS/WAXS and load–extension data.

Various sheet samples of isotropic polyethylene were obtained from BP Chemicals Ltd. The sheet samples were prepared by melt pressing at 200°C for 5 min followed by cooling at a rate of $\approx$ 15°C min^{-1}. The 0.5 mm thick sample that was used in the experiment that is reported here is a HDPE of $\overline{M}_{\mathrm{w}} = 320\,000$ with a density of 0.9496 g cm^{-3}. In order to be able to correlate both the X-ray data and local stress–strain information it is essential to be able to predict the region of the sample from which the deformation takes place. For this reason 'hourglass' profile samples were cut to ensure strain localization in the centre of the sample (sample length between jaws $\approx$ 10 mm, maximum sample width $\approx$ 10 mm, minimum sample width $\approx$ 5 mm). At the stage of sample mounting it is important to ensure that the centre of the beam is coincident with the narrowest region of the specimen. The sample was marked with 0.5 mm spaced horizontal lines to allow accurate local strain measurements to be performed by post-mortem analysis of the sample video data. Furthermore, by careful analysis of the video data it is possible to calculate the sample width and thickness and therefore the sample cross-section variation during the draw in the area of the sample from which the X-ray data was collected.

The HDPE sample was drawn at 35°C with an overall extension rate of $\approx$ 3 s^{-1}, although the local draw rate varies widely throughout the draw. The final draw ratio achieved was $\approx$ 7:1. The total experimental time was 2 s resulting in 50 consecutive 40 ms SAXS/WAXS patterns and simultaneous video strain data. All X-ray diffraction patterns that were analyzed were corrected for detector distortion[14] and detector response, and were calibrated using silicon powder and wet rat-tail collagen to determine the specimen to detector distance for the WAXS and SAXS data respectively. Several identical experiments were performed in order to establish the reproducibility of the experimental results. It was found that although there were some small differences in the variation of strain with draw time for different samples, the overall results that are obtained are very similar.

Results and discussion

Figure 2 shows selected 40 ms SAXS/WAXS frames that were collected during the draw, with the simultaneous sample video data inset. Frame timings are given in milliseconds from the onset of the draw and are taken as the centre of the 40 ms time frames. The WAXS data shown in *Figure 2* samples a maximum spacing range of 5.1–1.9 Å whilst the SAXS data samples a maximum range of 900–130 Å in this particular experimental arrangement. For the purpose of the calculation of the true stress–true strain behaviour, the series of sample video images were analyzed in detail to obtain both sample cross-section and strain data. *Figure 3* shows the true stress–true strain curve that was obtained. The stress–strain curve shows that there is a very distinct point at which the polymer yields, which occurs between 220 ms and 260 ms into the draw. There is no evidence of a double yield point as has been reported for HDPE samples in other studies[15], though this is likely to be due not to differences in the material but rather to a much higher strain rate regime.

The initial undeformed SAXS data consists of a largely isotropic ring of intensity, indicating that the undeformed sample is spherulitic in nature with a lamellar spacing of $\approx$ 350 Å. Some deviation from a purely isotropic ring is visible due to a small degree of pre-orientation in the sample as is common in melt pressed samples. The sequence of SAXS patterns shows a dramatic intensification after the initial stages of the draw. This is attributed to the formation of micro-voids in the material. It can be seen that the initial intensification occurs in the meridional regions but that further strain causes a gradual transfer of intensity into the equatorial regions. It is possible to account for the meridional intensification by considering that the initial production of cracks/voids occurs in the equatorial (with respect to the draw direction) regions of the spherulites and that they are elongated perpendicular to the draw direction. It has been suggested that the progression from this state is that either further voids are generated which are elongated parallel to the draw direction, or that the initial voids are gradually drawn out parallel to the draw direction[16]. In the data presented here, the meridional scattering appears to smoothly transfer totally from the meridian to the equator, therefore it appears that the latter model is the case. The onset of rapid meridional intensification and therefore void activation, occurs at 220 ms (strain, $\epsilon = 0.2$), which corresponds exactly to the yield point that is observed in the stress–strain curve. A consequence of the generation of micro-voids which can be seen in the sample video images, is the strong degree of whitening of the sample in the draw region.

The WAXS data highlights the extent and quality of data that can be collected using the technique described here. Prior to deformation the pattern shows that an unoriented orthorhombic crystal structure is present with the refined unit cell parameters $a = 7.39$ Å, $b = 5.02$ Å, $c = 2.59$ Å. The two intense inner reflections, which are indexed as (110) and (200), dominate the scattering although other reflections are visible at higher scattering angles. During the draw it can be seen that extra reflections appear in the pattern due to the onset of a stress-induced (Martensitic) partial orthorhombic to monoclinic phase change. In particular the appearance of an extra reflection inside the orthorhombic (110) reflection is noticeable. These extra

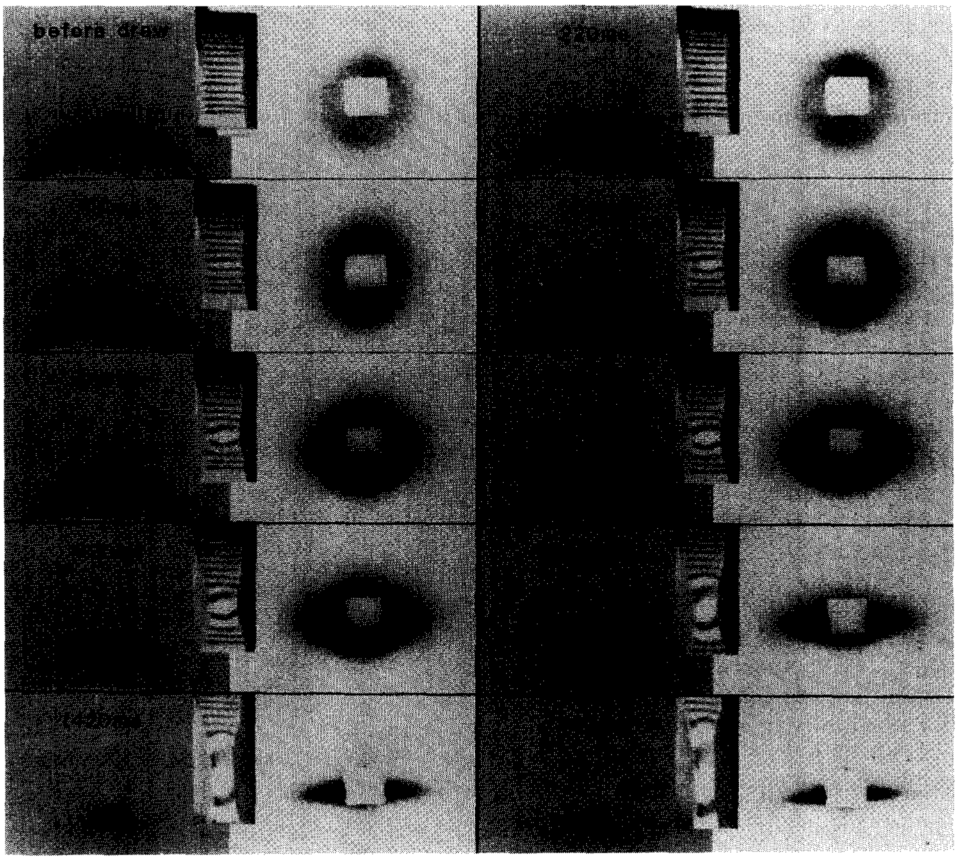

Figure 2 Selected pairs of simultaneous 40 ms WAXS and SAXS frames with the corresponding strain data inset. The frame timings that are given for each set of data relate to the time from the onset of the draw to the temporal centre of the data

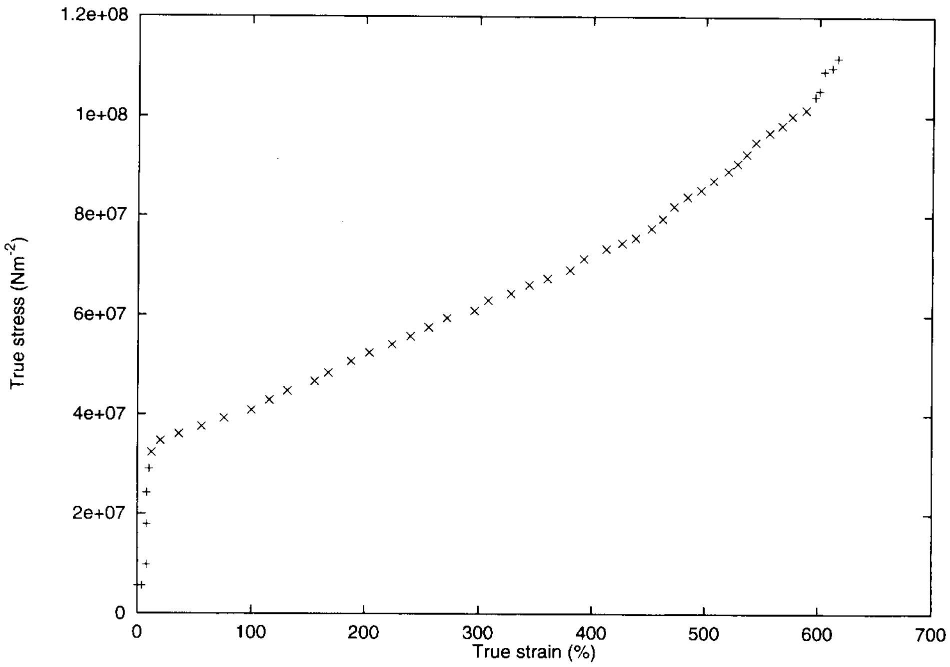

Figure 3 Plot of the true stress against true strain for the deformation of HDPE at 35°C: (+) orthorhombic phase only (apparent both in the early and very late stages of the deformation), (×) coexistence of orthorhombic and monoclinic phases (apparent in the intermediate stages of the deformation)

reflections correspond to a monoclinic phase with cell parameters $a = 8.09$ Å, $b = 2.53$ Å, $c = 4.79$ Å, $\beta = 107.9°$[17]. The extra reflection inside the orthorhombic (110) reflection indexes as the monoclinic (001). A study of the deformation of similar HDPE samples at significantly lower draw rates[18] suggests that the onset of the monoclinic phase occurs in parallel to the onset of voiding. From the WAXS data presented in *Figure 2* it is possible to establish the appearance of the (001) monoclinic reflection as occurring at 220 ms into the draw. The appearance of this phase is, however, temporary since at the end of the draw only a highly c-axis oriented orthorhombic crystal structure is present.

Conclusions

The technique for the collection of simultaneous SAXS/WAXS and true stress–strain data has proved to be a very useful tool for the study of the orientation mechanisms which occur in high-density polyethylene. The rate at which the data can be collected allows the polymer sample to be deformed at strain rates that are relevant for the study of impact behaviour. Further development of the understanding of the deformation mechanisms of polyethylene at high strain rates is currently under way. In particular it is essential to understand the effect of chain branching, strain rate, and deformation temperature.

Acknowledgements

This work was supported by EPSRC grant GR/J/86643 to WF, AM, J. Bordas and E. Towns-Andrews. We are grateful to J. Bordas and E. Towns-Andrews for advice on beamline design, A. Gleeson for technical support on beamline 16.1 and also G. Capaccio (BP Chemicals Ltd) for providing polyethylene samples. We thank Photonic Science Ltd, D. Bowyer, M. Daniels, M.G. Davies, G. Dudley, E.J.T. Greasley, G. Marsh, H. Lloyd, C. Sutton and M.P. Wallace for technical support and help with the preparation of the manuscript.

References

1. Bunn, C.W., *Trans. Faraday Soc.*, 1939, **35**, 482–491.
2. Hay, I.L. and Keller, A., *Kolloid-Z. Z. Polym.*, 1965, **204**, 43–74.
3. Hay, I.L. and Keller, A.J., *Polymer Sci. Part C*, 1970, **30**, 289–296.
4. Lin, L. and Argon, A.S., *J. Mater. Sci*, 1994, **29**, 294–323.
5. van Aerle, N.A.J.M. and Braam, A.W.M., *Colloid Polym. Sci.*, 1989, **267**(4), 323–329.
6. Gerasimov, V.I., Genin, Ya.V. and Tsvankin, D.Ya., *J. Polym. Sci. (Polym. Phys. Ed.)*, 1974, **12**, 2035–2046.
7. Wutz, C., Bark, M., Cronauer, J., Dohrmann, R. and Zachmann, H.G., *Rev. Sci. Instrum.*, 1995, **66**(2), 1303–1307.
8. Bras, W., Mant, G.R., Derbyshire, G.E., O'Kane, W.J., Helsby, W.I., Hall, C.J. and Ryan, A.J., *J. Synchrotron Rad.*, 1995, **2**, 87–92.
9. Hughes, D.J., Mahendrasingam, A., Heeley, E.L., Oatway, W.B., Martin, C., Towns-Andrews, E. and Fuller, W.J., *Synchrotron Rad.*, 1996, **3**, 84–90.
10. G'Sell, C., Hiver, J.M., Dahoun, A. and Souahi, A.J., *Mater. Sci.*, 1992, **27**, 5031–5039.
11. Francois, P., Gloaguen, J.M., Hue, B. and Lefebvre, J.M., *J. Phys. III France*, 1994, **4**, 321–329.
12. Mahendrasingam, A., Fuller, W., Forsyth, V.T., Oldman, R.J., MacKerron and Blundell, D., *Rev. Sci. Instrum.*, 1992, **63**, 1087–1090.
13. Blundell, D.J., MacKerron, D.H., Fuller, W., Mahendrasingam, A., Martin, C., Oldman, R.J., Rule, R.J. and Riekel, C., *Polymer*, 1996, **37**(15), 3303–3311.
14. Hammersley, A.P., Svensson, S.O. and Thompson, A., *Nucl. Instrum. Meth. Phys. Res. A*, 1994, **346**, 312–321.
15. Brooks, N.W., Duckett, R.A. and Ward, I.M., *Polymer*, 1992, **33**(9), 1872–1880.
16. Young, P., Kyu, T., Suehiro, S., Lin, J.S. and Stein, R.S., *J. Polym. Sci. (Polym. Phys. Ed.)*, 1983, **21**, 881–892.
17. Seto, T., Hara, T. and Tanaka, K., *Jpn. J. Appl. Phys.*, 1968, **7**(1), 31–42.
18. Butler, M.F., Donald, A.M., Bras, W., Mant, G.R., Derbyshire, G.E. and Ryan, A.J., *Macromol.*, 1995, **28**(19), 6383–6393.